

MULTIPLE-INPUT-PORT AND MULTIPLE-OUTPUT-PORT AMPLIFIER FOR WIRELESS RECEIVERS

Frédéric Broydé and Evelynne Clavelier

Excem — 12, chemin des Hauts de Clairefontaine — 78580 Maule — France
tel: +33 1 34 75 13 65 fax: +33 1 34 75 13 66 e-mail: fredbroyde@eurexcm.com

Abstract

This paper shows that interesting properties are obtained when the front-end of a wireless receiver using several antennas comprises a multiple-input-port and multiple-output-port (MIPMOP) amplifier, as opposed to multiple independent single-input-port and single-output-port low-noise amplifiers. The case of a receiver front-end implementing a MIMO series-series feedback amplifier (MIMO-SSFA) is presented in detail.

1. Introduction

Receivers for Multiple-Input and Multiple-Output (MIMO) or Single-Input and Multiple-Output (SIMO) wireless communication systems use several antennas forming a multiple-port antenna array. The performances of multiple-antenna radio communication systems are often assessed using the assumption of uncoupled antennas. This is clearly an approximation, which will fail if the antennas are close to each other. The physical size of the antenna array is often limited by the application, e.g. in the case of portable transceivers. There is consequently a need to take into account the effects of antenna separations in an array of antennas used as a multiport, and such effects are likely to impact the properties of a radio communication system and the design of the wireless receiver [1] [2] [3] [4].

This paper shows that a non-conventional wireless receiver front-end connected to an antenna array may provide improved performances compared to a conventional design. Two types of non-conventional wireless receiver front-end will be considered: passive and active. However, this paper focuses on active non-conventional wireless receiver front-ends of the MIMOmatch type, which by definition comprise a multiple-input-port and multiple-output-port (MIPMOP) amplifier.

A detailed design example will show how an active non-conventional wireless receiver front-end may be designed to obtain a given input impedance matrix, using a MIMO series-series feedback amplifier (MIMO-SSFA) [5] [6]. The resulting directivity will also be studied, in the context of a deterministic plane wave impinging on the antenna array used for reception.

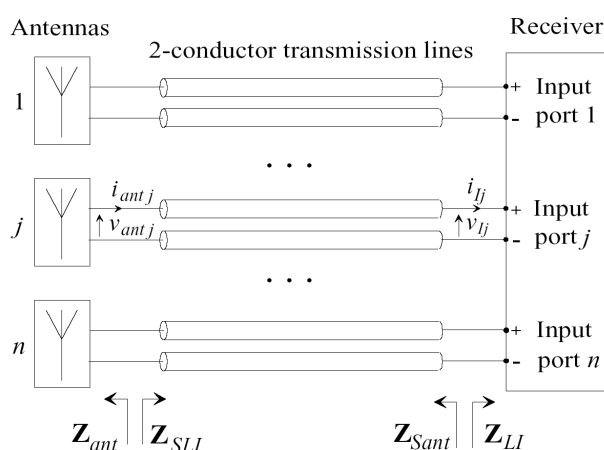


Fig. 1. An array of n antennas connected to n uncoupled 2-conductor transmission lines connected to a receiver having n input ports.

2. Conventional front-end design

A multiport array of antennas used for reception is shown in Fig. 1. The n uncoupled transmission lines linking the n antennas to the n input ports alter the impedance matrices seen by the receiver and the antenna. In order to characterize this structure, we define the following matrices: \mathbf{Z}_{ant} is the impedance matrix of the array of n antennas, \mathbf{Z}_{SLI} is the impedance matrix seen by the array of n antennas, \mathbf{Z}_{Sant} is the impedance matrix seen by the receiver, and \mathbf{Z}_{LI} is the input impedance matrix of the receiver.

Such an antenna array used for reception may be implemented in the conventional scheme for wireless reception shown in Fig. 2, comprising 4 antennas (100), 4 bandpass filters (200), 4 low-noise amplifiers (300), 4 analog processing and conversion circuits (400) and a multiple-input signal processing device (550), whose output is connected to the destination (600).

In Fig. 2, the analog processing and conversion circuits may implement the following main steps: frequency conversion, filtering and amplification of the intermediate frequency signal, demodulation and analog-to-digital conversion of the I and Q signals. The multiple-input signal processing device used in Fig. 2 for instance performs OFDM demodulation of each input signal, space-time

decoding (MIMO decoding), channel decoding and source decoding [3] [7] [8].

The receiver block of Fig. 1 corresponds to the items (200), (300), (400), (550) and (600) of Fig. 2, while the transmission lines between antennas and receivers are not shown in Fig. 2. \mathbf{Z}_{LI} (which relates to the input of the bandpass filters) is a diagonal matrix, because the band-pass filters (200) and the low-noise amplifiers (300) are uncoupled. For the same reason, \mathbf{Z}_{SLI} is also a diagonal matrix. On the other hand, the impedance matrix \mathbf{Z}_{ant} is not diagonal because the antennas are close to each other. \mathbf{Z}_{Sant} is not diagonal either. Consequently, no matching is possible between \mathbf{Z}_{ant} and \mathbf{Z}_{SLI} or between \mathbf{Z}_{Sant} and \mathbf{Z}_{LI} .

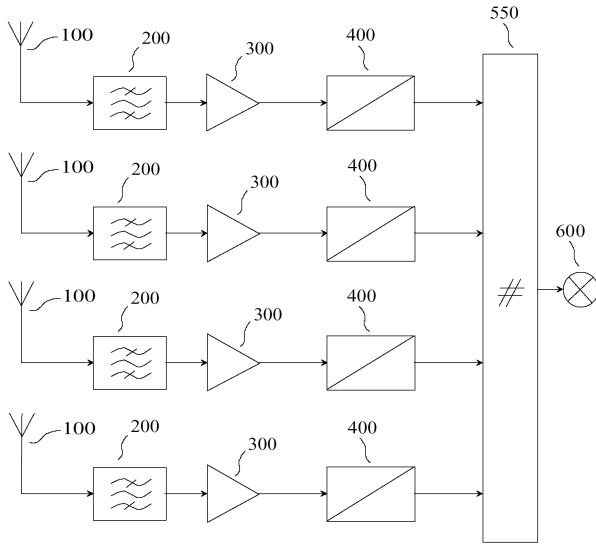


Fig. 2: A conventional 4-antenna wireless receiver.

In Fig. 2, we see 4 independent analog chains each consisting of the items 200, 300 and 400. A multiple-input-port receiver front-end is called a multiple-input-port and multiple-output-port (MIPMOP) front-end if it is not made of multiple independent analog chains.

3. Passive MIPMOP front-end design

The block diagram of a wireless receiver using a passive MIPMOP front-end is shown in Fig. 3, in which the front-end comprises a MIPMOP passive linear matching network (250), and other blocks mentioned in Fig. 2. The MIPMOP passive linear matching network used in Fig. 3 is also a band-pass filter. It may provide hermitian matching between \mathbf{Z}_{ant} and \mathbf{Z}_{SLI} .

Let us use \mathbf{X}^* to denote the hermitian adjoint of a matrix \mathbf{X} , that is to say a matrix equal to the matrix transpose of the matrix complex conjugate of \mathbf{X} . In this paper, we consider that hermitian matching is obtained if the input ports of the receiver see an impedance matrix \mathbf{Z}_{Sant} equal to the hermitian adjoint \mathbf{Z}_{LI}^* of the input impedance matrix \mathbf{Z}_{LI} of the receiver. Hermitian matching to an array of antennas

directly provides a stronger signal because it is a sufficient condition for maximum power transfer [9] [10]. It may eventually improve the signal-to-noise ratio, if noise is not degraded by the provisions providing conjugate matching, such as losses in the MIPMOP passive linear matching network. It has been shown that the degradation of performances caused by losses must be taken into account to obtain a realistic MIPMOP passive linear matching network design [11] [12]. Also, MIPMOP passive linear matching network are complex since $n(2n+1)$ high-Q reactive two-terminal circuit elements are required. They are therefore not yet used in practice.

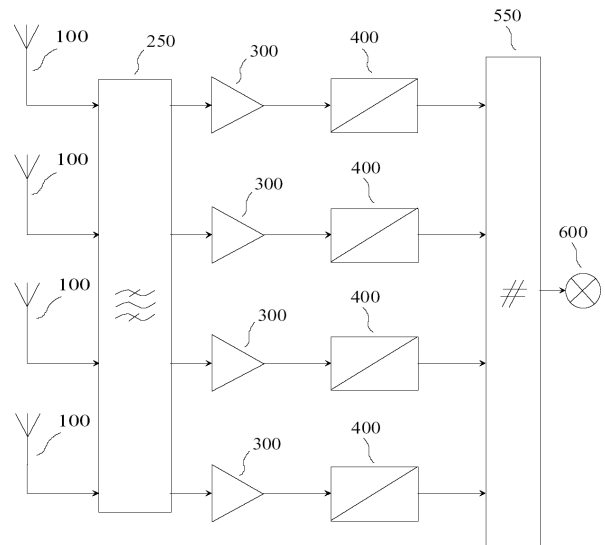


Fig. 3: A 4-antenna wireless receiver using a passive MIPMOP front-end design.

We refer to the scheme of Fig. 3 as a passive MIPMOP design because couplings between the inputs of the receiver are caused by a passive filter. In addition to power transfer, other important characteristics of a front-end design are the directional patterns and the correlation coefficients of the signals reaching the multiple-input signal processing device (550). Since this paper is focused on electronic design, we will not discuss these parameters which are closely related to the properties of antennas and to propagation models.

4. Active MIPMOP front-end design

Figure 4 shows a block diagram of a MIMO wireless receiver using an active MIPMOP front-end design, comprising a MIPMOP low-noise amplifier (350), and the other blocks used in Fig. 2. The motivations of this architecture lie in the following observations:

- in Fig. 3, the potential benefits of introducing couplings before the low noise amplifier are offset by increased losses in the passive linear matching network;
- however, it is possible to introduce couplings inside the

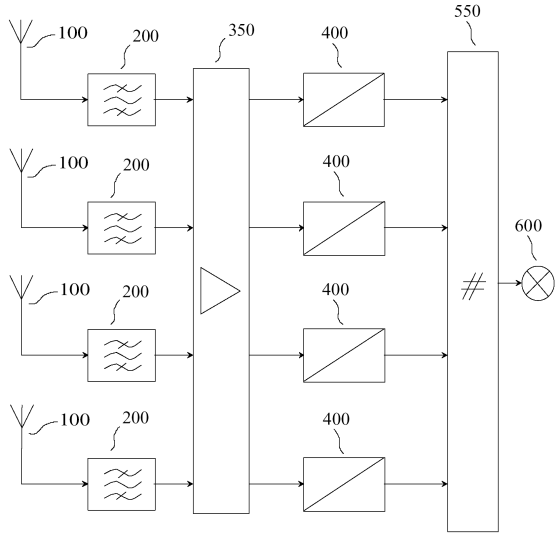


Fig. 4: A 4-antenna wireless receiver using an active MIPMOP front-end design.

amplifier, so as to obtain hermitian matching without significant added noise;

■ a good building block for this approach is the MIMO series-series feedback amplifier (MIMO-SSFA) initially introduced to obtain reduced crosstalk and echo in multiconductor interconnections [5].

Figure 5 shows a MIMO-SSFA, having $n = 4$ signal input terminals and n signal output terminals, comprising n active sub-circuits (ASC) and a feedback network. Using j to denote an integer such that $1 \leq j \leq n$, Fig. 6 shows the ASC j having its sub-circuit input terminal I connected to the signal input terminal j and its sub-circuit output terminal O connected to the signal output terminal j .

Using the notations of Fig. 6, we require that each ASC is such that i_{CAj} and i_{OAJ} depend on $e_j - w_j$. An ASC can be a single transistor or a more complex circuit possibly having connections to ground and/or to one or more power supplies, even though such connections are not shown. The feedback network has a grounded terminal and n other terminals each being connected to the sub-circuit common terminal of a different ASC. The feedback network presents a non-diagonal impedance matrix \mathbf{Z}_{FB} , this impedance matrix being defined with respect to the reference terminal, and the feedback network produces a negative feedback. The name “MIMO-SSFA” used to designate this amplifier is a consequence of the fact that the negative feedback used in Fig. 5 can be considered as a generalization of series-series feedback. We further require that the feedback network cannot be split into two uncoupled sub-networks.

We define the input current i_{Ij} flowing into the signal input terminal j and the input voltage v_{Ij} between the signal input terminal j and ground. We define the column-vector \mathbf{I}_I of the input currents i_{I1}, \dots, i_{In} , and the column-vector \mathbf{V}_I of the input voltages v_{I1}, \dots, v_{In} . We define the output current i_{Oj} flowing into the signal output terminal j and the output voltage v_{Oj} between the signal output terminal j and ground. We define the column-vector \mathbf{I}_O of the output

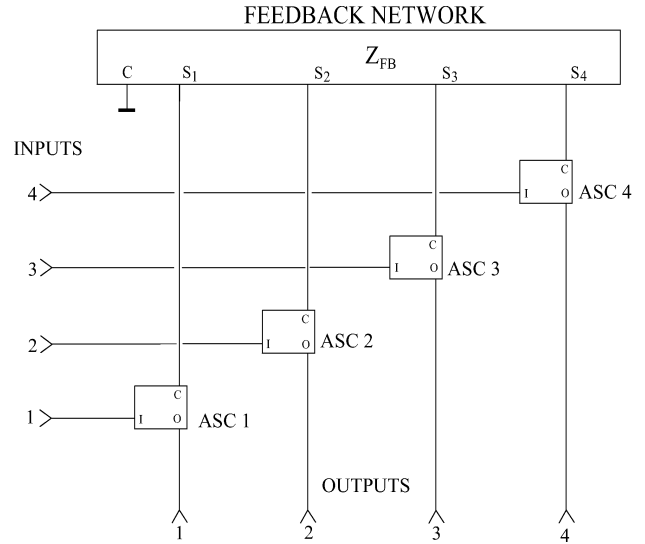


Fig. 5: A MIMO series-series feedback amplifier (MIMO-SSFA).

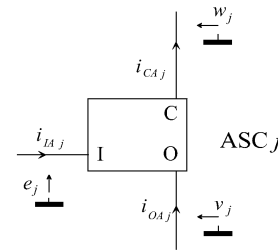


Fig. 6: An active sub-circuit (ASC) of the MIMO-SSFA.

currents i_{O1}, \dots, i_{On} , and the column-vector \mathbf{V}_O of the output voltages v_{O1}, \dots, v_{On} .

For small signals, at a given quiescent operating point, the MIMO-SSFA is characterized, in frequency domain, by the two following equations:

$$\mathbf{I}_I = \mathbf{Y}_{ISS} \mathbf{V}_I + \mathbf{Y}_{RSS} \mathbf{V}_O \quad (1)$$

$$\mathbf{I}_O = \mathbf{Y}_{TSS} \mathbf{V}_I + \mathbf{Y}_{OSS} \mathbf{V}_O \quad (2)$$

where we can refer

- to \mathbf{Y}_{ISS} as the “short-circuit input admittance matrix” of the MIMO-SSFA or simply as the “input admittance matrix” when no confusion may occur,
- to \mathbf{Y}_{RSS} as the “short-circuit reverse transfer admittance matrix” of the MIMO-SSFA or simply as the “reverse transfer admittance matrix” when no confusion may occur,
- to \mathbf{Y}_{TSS} as the “short-circuit forward transfer admittance matrix” of the MIMO-SSFA or simply as the “transfer admittance matrix” when no confusion may occur, and
- to \mathbf{Y}_{OSS} as the “short-circuit output admittance matrix” of the MIMO-SSFA or simply as the “output admittance matrix” when no confusion may occur.

These four matrices have complex components and may be frequency-dependent. When an ASC j has only three terminals, the small-signal behavior of the ASC j may be described by the admittance matrix \mathbf{Y}_{TPj} of the two-port with respect to the sub-circuit common terminal, defined by

$$\begin{pmatrix} i_{IAj} \\ i_{OAj} \end{pmatrix} = \mathbf{Y}_{TPj} \begin{pmatrix} e_j - w_j \\ v_j - w_j \end{pmatrix} \quad (3)$$

where

$$\mathbf{Y}_{TPj} = \begin{pmatrix} y_{TP11j} & y_{TP12j} \\ y_{TP21j} & y_{TP22j} \end{pmatrix} \quad (4)$$

In order to provide simpler formulas, we will assume that all active sub-circuits have substantially identical properties. Dropping the j indices, for ASC having exactly 3 terminals, we get [6]:

$$\mathbf{Y}_{ISS} = \left[y_{TP11} \mathbf{1}_n + \{y_{TP11}y_{TP22} - y_{TP12}y_{TP21}\} \mathbf{Z}_{FB} \right] \times \left[\mathbf{1}_n + (y_{TP11} + y_{TP12} + y_{TP21} + y_{TP22}) \mathbf{Z}_{FB} \right]^{-1} \quad (5)$$

$$\mathbf{Y}_{RSS} = \left[y_{TP12} \mathbf{1}_n - \{y_{TP11}y_{TP22} - y_{TP12}y_{TP21}\} \mathbf{Z}_{FB} \right] \times \left[\mathbf{1}_n + (y_{TP11} + y_{TP12} + y_{TP21} + y_{TP22}) \mathbf{Z}_{FB} \right]^{-1} \quad (6)$$

$$\mathbf{Y}_{TSS} = \left[y_{TP21} \mathbf{1}_n - \{y_{TP22}y_{TP11} - y_{TP12}y_{TP21}\} \mathbf{Z}_{FB} \right] \times \left[\mathbf{1}_n + (y_{TP11} + y_{TP12} + y_{TP21} + y_{TP22}) \mathbf{Z}_{FB} \right]^{-1} \quad (7)$$

$$\mathbf{Y}_{OSS} = \left[y_{TP22} \mathbf{1}_n + \{y_{TP11}y_{TP22} - y_{TP12}y_{TP21}\} \mathbf{Z}_{FB} \right] \times \left[\mathbf{1}_n + (y_{TP11} + y_{TP12} + y_{TP21} + y_{TP22}) \mathbf{Z}_{FB} \right]^{-1} \quad (8)$$

where $\mathbf{1}_n$ is the identity matrix of size $n \times n$. Using (5)-(8), it is possible to proportion the ASC and the impedance matrix \mathbf{Z}_{FB} of the feedback network to obtain wanted interactions between the channels. In addition, input filters and output filters may also be used to further tailor the input admittance matrix \mathbf{Y}_{LI} of the receiver. In the following, we will use n uncoupled input filters and n uncoupled output filters connected to the MIMO-SSFA to obtain the filters (200) and the MIPMOP amplifier (350) shown in Fig. 4.

5. Design example using 4 antennas

A. Description of the antenna array

This section applies to a circular array of four parallel half-wave dipole antennas (side-by-side configuration) for $f_0 = 1880$ MHz presenting a $0.424 \lambda = 27$ mm spacing between the nearest array elements. Each dipole presents a self-impedance equal to 73.13Ω [13, pp. 34-37] and the mutual impedances are computed with the induced EMF method, using a closed-form formula for the fields and a numerical integration [14, eq. 8-68]. The impedance matrix of the antenna array is computed as

$$\mathbf{Z}_{ant} = \begin{pmatrix} 73.1 & 1.1-36.4j & -23.3-15.9j & 1.1-36.4j \\ 1.1-36.4j & 73.1 & 1.1-36.4j & -23.3-15.9j \\ -23.3-15.9j & 1.1-36.4j & 73.1 & 1.1-36.4j \\ 1.1-36.4j & -23.3-15.9j & 1.1-36.4j & 73.1 \end{pmatrix} \Omega \quad (9)$$

If a plane wave of wave vector \mathbf{k} , having a linear polarization along the unit vector \mathbf{u} such that $\mathbf{u} \cdot \mathbf{k} = 0$ is impinging on the antenna array, the open-circuit voltage v_{antOj} of the antenna j is given by [13, p. 305] [15, p. 6-5]:

$$v_{antOj} = H_{effj} E_0 \exp(-j\mathbf{k} \cdot \mathbf{r}_j) \quad (10)$$

where E_0 is the magnitude of the incident electric field at the origin, \mathbf{r}_j is the radius vector of the center of the antenna j , where the effective height H_{effj} is

$$H_{effj} = \frac{c_0}{\pi f_0} \frac{\cos\left(\frac{\pi}{2} \cos\theta\right)}{\sin\theta} \mathbf{u} \cdot \mathbf{e}_\theta \quad (11)$$

where c_0 is the free-space light velocity and \mathbf{e}_θ is the unit vector of the spherical coordinates corresponding to partial derivation with respect to the zenith angle θ . For $\theta = \pi/2$ and $|\mathbf{u} \cdot \mathbf{e}_\theta| = 1$, the effective height is 51 mm at $f_0 = 1880$ MHz.

We assume that each antenna is connected to the MIPMOP amplifier via a two-conductor interconnection (for instance a coaxial cable) behaving as a two-conductor transmission line. The antenna number j is connected to the near-end of the interconnection number j of length d_j , characteristic impedance z_{Cj} , phase velocity c_j and attenuation constant α_j . The far-end of the interconnection number j is connected to the input port number j of the MIPMOP amplifier. Let us define the characteristic impedance matrix \mathbf{Z}_C of the interconnection as

$$\mathbf{Z}_C = \text{diag}_n(z_{C1}, \dots, z_{Cn}) \quad (12)$$

where $\text{diag}_n(x_1, \dots, x_n)$ denotes the diagonal matrix of size $n \times n$ of the components x_1, \dots, x_n . Let us also define the transmission matrix \mathbf{T} of the interconnections as

$$\mathbf{T} = \text{diag}_n \left(e^{-[\alpha_1 + j \frac{2\pi f_0}{c_1}] d_1}, \dots, e^{-[\alpha_n + j \frac{2\pi f_0}{c_n}] d_n} \right) \quad (13)$$

After some derivation, we get

$$\mathbf{Z}_{Sant} = \left\{ \frac{\mathbf{T} + \mathbf{T}^{-1}}{2} \mathbf{Z}_{ant} - \frac{\mathbf{T} - \mathbf{T}^{-1}}{2} \mathbf{Z}_C \right\} \left\{ \frac{\mathbf{T} + \mathbf{T}^{-1}}{2} \mathbf{Z}_C - \frac{\mathbf{T} - \mathbf{T}^{-1}}{2} \mathbf{Z}_{ant} \right\}^{-1} \mathbf{Z}_C \quad (14)$$

If we assume that four identical 0.045-meter-long transmission lines are used, having, at $f_0 = 1880$ MHz, a propagation velocity of $0.5 c_0$, a characteristic impedance of 80Ω and an attenuation of 2.0 dB/m, the resulting impedance matrix seen by the receiver at f_0 is equal to:

$$\mathbf{Z}_{Sant} = \begin{pmatrix} 84.4+10.1j & -18.7-32.5j & -17.9+13.5j & -18.7-32.5j \\ -18.7-32.5j & 84.4+10.1j & -18.7-32.5j & -17.9+13.5j \\ -17.9+13.5j & -18.7-32.5j & 84.4+10.1j & -18.7-32.5j \\ -18.7-32.5j & -17.9+13.5j & -18.7-32.5j & 84.4+10.1j \end{pmatrix} \Omega \quad (15)$$

We note that, when we compare (9) and (15), the relative difference between diagonal entries is small, but the non-diagonal entries are thoroughly modified.

B. Design of a MIPMOP low-noise amplifier

In this section we wish to synthesize a MIPMOP amplifier corresponding to the blocks (200) and (350) of Fig. 4, such that $\mathbf{Z}_{Sant} = \mathbf{Z}_{LI}^*$, i.e. such that hermitian matching is obtained. The selected MIPMOP amplifier structure is shown in Fig. 7, where a MIMO-SSFA is used. Each ASC is made of a packaged low-noise pseudomorphic HEMT and a drain resistor providing resistive loading to improve stability. The feedback network of the MIMO-SSFA consists of the 4 inductors L411 to L414, coupled by mutual induction.

If mutual induction was not present, Fig. 7 would represent four independent single-input and single-output LNA with inductive source degeneration. Such LNA are capable of simultaneously providing minimum noise figure and conjugate matching to uncoupled antennas [16] [17]. In our active MIPMOP front-end design, mutual induction in the amplifier produces a non-diagonal input impedance matrix \mathbf{Z}_{LI} . Consequently, this low-noise MIPMOP amplifier requires no added circuit element compared to the four independent LNA used in the conventional design of Fig. 2.

We assume that the input impedance of each analog processing and conversion circuits (400) is 50Ω . Each of the 4 uncoupled output filters is made of an inductor (L511, etc) and a capacitor (C521, etc). The multiport load seen by the MIMO-SSFA looking into the output filter is characterized by a diagonal matrix \mathbf{Z}_{LSS} . The loaded input admittance matrix \mathbf{Y}_{LISS} of the MIMO-SSFA (i.e. the input impedance with \mathbf{Z}_{LSS} at the output, as opposed to \mathbf{Y}_{ISS} defined above) can then be computed as

$$\begin{aligned} \mathbf{Y}_{LISS} &= \mathbf{Y}_{ISS} - \mathbf{Y}_{RSS} (\mathbf{1}_m + \mathbf{Z}_{LSS} \mathbf{Y}_{OSS})^{-1} \mathbf{Z}_{LSS} \mathbf{Y}_{TSS} \\ &= \mathbf{Y}_{ISS} - \mathbf{Y}_{RSS} \mathbf{Z}_{LSS} (\mathbf{1}_m + \mathbf{Y}_{OSS} \mathbf{Z}_{LSS})^{-1} \mathbf{Y}_{TSS} \end{aligned} \quad (16)$$

where \mathbf{Y}_{ISS} , \mathbf{Y}_{RSS} , \mathbf{Y}_{TSS} and \mathbf{Y}_{OSS} are computed using (5)-(8) and equations corresponding to a SPICE model of the HEMT including package parasitics. Each of the 4 uncoupled input filters is made of an inductor (L221, etc) and a capacitor (C211, etc). The input impedance matrix \mathbf{Z}_{LI} of the MIPMOP amplifier is the input impedance matrix of these filters loaded by \mathbf{Y}_{LISS} . In this way, we obtain a set of closed-form expressions for \mathbf{Z}_{LI} . A similar approach provides a set of closed-form expression for the voltage gain matrix \mathbf{G}_V of the MIPMOP amplifier.

Because of the circular symmetry of our design, for given inductance and quality factor of L411 and a given value of R311, we need only to determine the values of the circuit elements C211, L221, C521, L511, and the values of the coupling coefficients k12 and k13. Through a step-by-step optimization process, we were able to obtain physically meaningful values for which $\|\mathbf{Z}_{LI} - \mathbf{Z}_{Sant}^*\|_2 = 0.178$ at the frequency 1880 MHz, where $\|\mathbf{X}\|_2$ denotes the Euclidian norm of \mathbf{X} . In other words, we could synthesize a MIPMOP amplifier providing an input impedance matrix \mathbf{Z}_{LI} which closely approximates \mathbf{Z}_{Sant} .

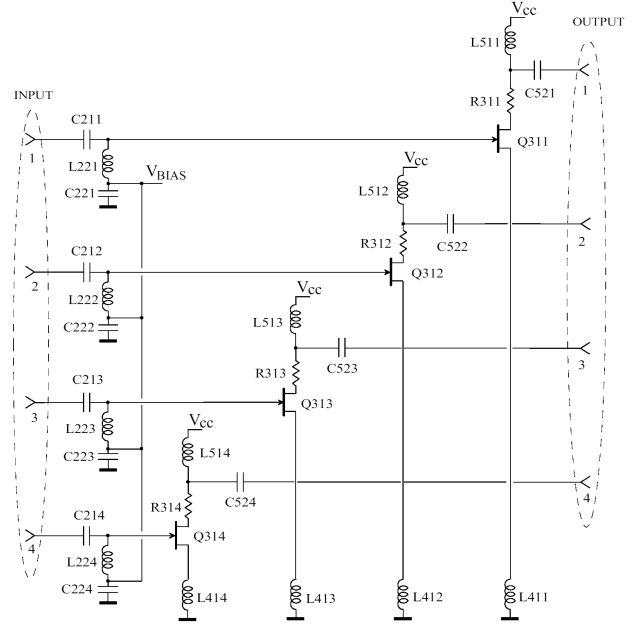


Fig. 7: A low-noise MIPMOP amplifier comprising a MIMO-SSFA, 4 independent input matching networks and 4 independent output matching networks.

At 1880 MHz, the computed voltage gain matrix of the amplifier is

$$\mathbf{G}_V = \begin{pmatrix} -2.8 - 3.3j & 0.1 + 0.9j & 0.2 + 0.4j & 0.1 + 0.9j \\ 0.1 + 0.9j & -2.8 - 3.3j & 0.1 + 0.9j & 0.2 + 0.4j \\ 0.2 + 0.4j & 0.1 + 0.9j & -2.8 - 3.3j & 0.1 + 0.9j \\ 0.1 + 0.9j & 0.2 + 0.4j & 0.1 + 0.9j & -2.8 - 3.3j \end{pmatrix} \quad (17)$$

and Fig. 8 shows the absolute value of the entries of \mathbf{G}_V and its L_1 norm, in dB, as a function of the frequency.

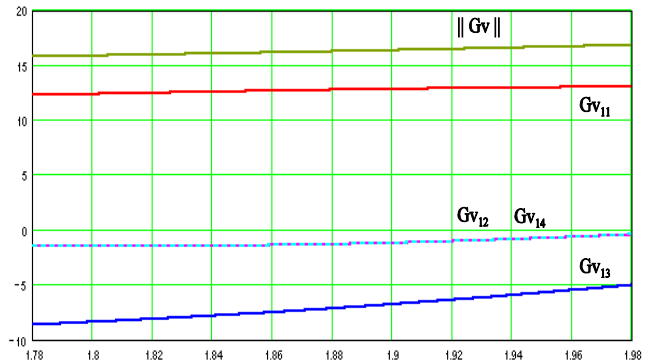


Fig. 8: Voltage gains (in dB) of the voltage gain matrix

We also computed the average power delivered to each analog processing and conversion circuits (400) and the mean of the average powers, at 1880 MHz, as a function of the azimuth angle. We used (10) and (11) to obtain the open-circuit voltages of the antennas. The results are shown in Fig. 9

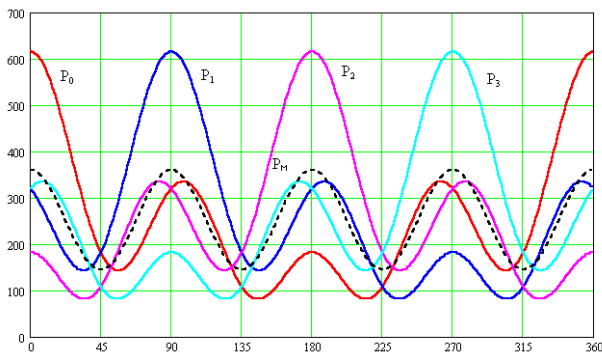


Fig.9: The average powers P_0 , P_1 , P_2 , and P_3 delivered by the outputs of the MIPMOP amplifier shown in Fig. 7 (in μW) and their mean $P_M = (P_0 + P_1 + P_2 + P_3)/4$ as a function of the azimuth (in degree) when the antenna array receives an incident plane wave of 1 V/m (peak).

6. Conclusion

A receiver front-end comprising a MIPMOP amplifier (MIMOmatch front-end) may provide a wanted non-diagonal load impedance matrix to an array of antennas. In the theoretical example studied in this paper, nearly maximum power transfer from the antenna array to the receiver was obtained without any additional part compared to a conventional design, since mutual induction between the degeneration inductors provided the coupling.

A full design would also take into account the correlations between the different channels, and noise. Using some assumptions (for instance 2-dimensional Rayleigh channels), correlation coefficients between the channels may easily be computed and taken into account in the design. The question regarding noise is more difficult, both from the measurement and from the theoretical standpoints, because of the couplings in the amplifier and in the antenna array. However, the influence of mutual impedances between antennas is, as far as we know, always disregarded in the noise characterization of a conventional receiver such as the one shown in Fig. 2. This is because standard approaches disregard the fact that the noise delivered by an input port may excite other input ports via antenna coupling. Consequently, we observe that suitable accepted noise parameters are not yet available [18].

We have shown that an active MIPMOP front-end should be considered when designing receivers using multiple antennas with narrow spacing. The design will require cooperation between the front-end and antenna designers since the interface specification is not as simple as “50 Ω ” anymore. Thus, co-design will provide the best performances, at no additional manufacturing cost.

References

[1] R. Vaughan, N. Scott, “Closely spaced terminated monopoles for vehicular diversity antennas”, *Digest of the 1992 IEEE Antennas and Propagation Society International Symposium*, vol.2, pp. 1093-1096, 18-25 July 1992.

[2] J.W. Wallace, M.A. Jensen, A.L. Swindlehurst, B.D. Jeffs, “Experimental characterization of the MIMO wireless channel: data acquisition and analysis”, *IEEE Trans. Wireless Commun.*, vol. 2, No. 2, pp. 335-343, March 2003.

[3] M.A. Jensen, J.W. Wallace, “A review of antennas and propagation for MIMO wireless communications”, *IEEE Trans. Antennas Propagat.*, vol. 52, No. 11, pp. 2810-2824, Nov. 2004.

[4] Jesper Thaysen, Kaj. B. Jakobsen, “Multiple Antennas Arm Effective MIMO Systems”, *Microwave & RF*, pp. 65-78, May 2007.

[5] F. Broyd , E. Clavelier, “A simple method for transmission with reduced crosstalk and echo”, *Proc. 13th IEEE Int. Conf. on Electronics, Circuits and Systems*, ICECS 2006, pp. 684-687, Dec. 10-13, 2006.

[6] F. Broyd , E. Clavelier, “MIMO series-series feedback amplifiers”, to be published in *IEEE Trans. Circuit Syst. II*.

[7] G.L. St ber *et al*, “Broadband MIMO-OFDM Wireless Communications”, *Proceedings of the IEEE*, Vol. 92, No. 2, February 2004, pp. 271-294.

[8] J. Mietzner, P.A. Hoeher, “Boosting the Performance of Wireless Communication Systems: Theory and Practice of Multiple-Antenna Techniques”, *IEEE Commun. Mag.*, Vol. 42, No. 10, Oct. 2004, pp. 40-47.

[9] C.A. Desoer, “The Maximum Power Transfer Theorem for n -Ports”, *IEEE Trans. Circuit Theory*, vol. 20, No. 3, pp. 328-330, May 1973.

[10] M. Vidyasagar, “Maximum Power Transfer in n Ports With Passive Loads”, *IEEE Trans. Circuit Theory*, vol. 21, No. 3, pp. 327-330, May 1974.

[11] J. Weber, C. Volmer, K. Blau, R. Stephan, M.A. Hein, “Miniaturization of Antenna Arrays for Mobile Communications”, *Proc. 35th European Microwave Conf.*, Paris, France, Oct. 2005, pp. 1173-1176.

[12] J. Weber, C. Volmer, K. Blau, R. Stephan, M.A. Hein, “Miniaturized Antenna Arrays Using Decoupling Networks With Realistic Elements”, *IEEE Trans. Microwave Theory Tech.*, vol.54, No. 6, June 2006, pp. 2733-2740.

[13] R.E. Collin, *Antennas and Radiowave propagation*, International Edition, New York:McGraw-Hill, 1985.

[14] C.A. Balanis, *Antenna Theory, Analysis and Design*, second edition, John Wiley & Sons, Inc, 1997.

[15] Y.T. Lo, S.W. Lee, *Antennas Handbook, Volume II, Antenna theory*, New York:Van Nostrand Reinhold, 1993.

[16] J. Engberg, “Simultaneous input power match and noise optimization using feedback”, *Dig. Tech. Pap. Fourth European Microwave Conference*, Montreux, Sept. 1974, pp. 385-389.

[17] R.E. Lehmann, D.D. Heston, “X-Band Monolithic Series Feedback LNA”, *IEEE Trans. Microwave Theory Tech.*, vol. MTT-33, No. 12, December 1985, pp. 1560-1566.

[18] J. Randa, “Noise characterization of multiport amplifiers”, *IEEE Trans. Microwave Theory Tech.*, vol. 49, No. 10, Oct. 2001, pp. 1757-1763.

About the Authors



Fr d ric Broyd  received the “ing nieur” degree in physics engineering from the physical engineering department of the Ecole Nationale Sup rieure d’Ing nieurs Electriciens de Grenoble (ENSIEG), in 1984, and the Ph.D. in microwaves and microtechnologies from the Universit  des Sciences et Technologies de Lille (USTL), in 2004. He co-founded the Excem corporation in May 1988. Dr. Broyd  supervises the engineering and R&D projects of Excem.

Evelyne Clavelier received the “ing nieur” degree in physics engineering from the physical engineering department of the ENSIEG, in 1984. She co-founded the Excem corporation.

F. Broyd  and E. Clavelier are senior members of the IEEE. A bibliography of F. Broyd  and E. Clavelier, comprising more than 60 papers and 30 patents, and the full text of many papers may be accessed at <http://www.eurexcm.com>.